

Article

Dynamical Analysis and Sliding Mode Controller for the New 4D Chaotic Supply Chain Model Based on the Product Received by the Customer

Muhamad Deni Johansyah ^{1,*}, Sundarapandian Vaidyanathan ², Aceng Sambas ^{3,4}, Khaled Benkouider ⁵,
Seyed Mohammad Hamidzadeh ⁶ and Monika Hidayanti ¹

- ¹ Department of Mathematic, Universitas Padjadjaran, Jatinangor, Sumedang 45363, Indonesia; monika.hidayanti@unpad.ac.id
- ² Centre for Control System, Vel Tech University, Chennai 600062, Tamil Nadu, India; sundar@veltech.edu.in
- ³ Faculty of Informatics and Computing, Universiti Sultan Zainal Abidin, Besut 22200, Terengganu, Malaysia; acengsambas@unisza.edu.my or acengs@umtas.ac.id
- ⁴ Department of Mechanical Engineering, Universitas Muhammadiyah Tasikmalaya, Tasikmalaya 46196, Indonesia
- ⁵ Department of Electronics, Faculty of Technology, Badji-Mokhtar University, B.P. 12, Sidi Ammar, Annaba 23000, Algeria; benkouider.khaled@gmail.com
- ⁶ Department of Electrical Engineering, Khorasan Institute of Higher Education, Mashhad 91898, Iran; s.m.hamidzadeh@khorasan.ac.ir
- * Correspondence: muhamad.deni@unpad.ac.id

Abstract: Supply chains comprise various interconnected components like suppliers, manufacturers, distributors, retailers, and customers, each with unique variables and interactions. Managing dynamic supply chains is highly challenging, particularly when considering various sources of risk factors. This paper extensively explores dynamical analysis and multistability analysis to understand nonlinear behaviors and pinpoint potential risks within supply chains. Different phase portraits are used to demonstrate the impact of various factors such as transportation risk, quality risk, distortion, contingency reserves, and safety stock on both customers and retailers. We introduced a sliding mode control method that computes the sliding surface and its derivative by considering the error and its derivative. The equivalent control law based on the sliding surface and its derivative is derived and validated for control purposes. Our results show that the controller SMC can significantly enhance supply chain stability and efficiency. This research provides a robust framework for understanding complex supply chain dynamics and offers practical solutions to enhance supply chain resilience and flexibility.

Keywords: supply chain management; chaotic system; multistability; sliding mode control

MSC: 65P20; 26A33; 34A34; 65L07; 65L06; 93C40



Citation: Johansyah, M.D.; Vaidyanathan, S.; Sambas, A.; Benkouider, K.; Hamidzadeh, S.M.; Hidayanti, M. Dynamical Analysis and Sliding Mode Controller for the New 4D Chaotic Supply Chain Model Based on the Product Received by the Customer. *Mathematics* **2024**, *12*, 1938. <https://doi.org/10.3390/math12131938>

Academic Editor: José Roberto Castilho Piqueira

Received: 23 May 2024
Revised: 17 June 2024
Accepted: 19 June 2024
Published: 22 June 2024



Copyright: © 2024 by the authors. Licensee MDPI, Basel, Switzerland. This article is an open access article distributed under the terms and conditions of the Creative Commons Attribution (CC BY) license (<https://creativecommons.org/licenses/by/4.0/>).

1. Introduction

Initially, supply chain management focused on linear and deterministic models to optimize operations [1,2]. However, as businesses encountered increasing complexity and unpredictability, researchers began to recognize the limitations of these traditional approaches. Chaos theory provided a framework for understanding the nonlinear dynamics and emergent behaviors inherent in supply chain systems [3,4]. Studies identified chaotic behavior in various aspects of supply chain operations, including demand forecasting [5], inventory management [6], production scheduling [7], and distribution logistics [8]. These findings highlighted the need for new methodologies capable of managing and controlling the inherent chaos within supply chains [9,10].

In addressing the intricacies of supply chains, certain academics have utilized nonlinear dynamics theory to investigate pertinent issues. Ref. [11] introduced a pricing game model for a closed-loop supply chain system, involving a manufacturer and a retailer with distinct rationalities. Ref. [12] analyzed a three-dimensional mathematical model of supply chains, with the goal of stabilizing chaotic behavior. This involved introducing a linear control parameter to manage production levels and mitigate the risk of potential collapse, which could lead to dangerous instability. Ref. [13] explored the emergence of chaos within multi-level supply chains and provided insights into managing relevant factors to mitigate or eliminate system chaos. Ref. [14] investigated the dynamic behavior of a three-tier supply chain and devised an adaptive algorithm to counteract irregular dynamics stemming from uncertainties. Ref. [15] proposed a novel supply chain model considering non-monotonic demand variations with inventory levels and discussed synchronization phenomena in coupled supply chain models under both unidirectional and bidirectional coupling. Ref. [16] addressed the synchronization issue in supply chain systems using an active and adaptive integral sliding mode control method. Despite the existing literature, there remains limited discussion of dynamical analysis in 4D supply chain management. Thus, further research is warranted to explore studies concerning supply chains in 4D systems.

Chaos control associated with complex phenomena has been identified in actual supply chain systems. Numerous researchers have explored control and synchronization methods to characterize these systems in the literature such as robust control [9], delayed feedback control [17], adaptive sliding mode control [18], ANN [19], ANFIS [20], Robust H_∞ control [21], tracking control [22], stochastic fixed-time tracking control [23], fuzzy neural network control [24], and nonlinear control [25].

Studying the SMC for the new 4D CSCM based on the product received by the customer is important because it enhances the stability and control of complex, nonlinear supply chain behaviors, ensuring smooth and predictable operations [26]. The SMC effectively mitigates risks such as transportation delays, quality fluctuations, and information distortion by dynamically adjusting system parameters, reducing disruptions [27]. This leads to improved supply chain performance, including better inventory management, reduced lead times, and optimized resource utilization, resulting in increased efficiency and cost savings. The controller's adaptability to real-time changes ensures the supply chain remains resilient in the face of unexpected fluctuations. Additionally, the SMC manages coexisting attractors, steering the system towards desirable states and avoiding undesirable outcomes. Practical applications of the SMC translate into better forecasting, inventory control, and risk management, maintaining competitive advantage [28]. This study bridges the gap between advanced control theory and practical supply chain dynamics, providing valuable insights and opening new avenues for research and application. The validation of the SMC through simulations demonstrates its potential in handling complex supply chain issues and provides confidence in its practical deployment.

In the dynamic landscape of supply chain management, the emergence of chaos theory has shed light on the complex and unpredictable behavior inherent in supply chain systems. With the recognition of chaotic dynamics within supply chains, there arises a need to explore novel control strategies capable of navigating this intricate environment effectively. This project focused on addressing this challenge through the development of a sliding mode controller for a new 4D CSCM, specifically centered on the product received by the customer.

The integration of chaos theory into supply chain dynamics underscores the existence of coexisting attractors. Understanding and controlling these attractors are crucial for ensuring stability and optimizing performance in supply chain operations. By leveraging the insights from chaos theory and employing advanced control techniques such as sliding mode control, this project aimed to design a control framework capable of managing the complex dynamics of the supply chain model.

The main contributions and novelty of this paper include investigating the dynamics of the new 4D CSCM based on the product received by the customer, identifying and

characterizing coexisting attractors within the supply chain system, developing a sliding mode control strategy to regulate the system dynamics and stabilize the supply chain operation, and evaluating the performance and efficacy of the proposed sliding mode controller through simulation and validation studies.

This work is organized as follows. The next section presents the introduction and objectives of the study. In Section 2, we derive the new 4D CSCM based on the product received by the customer. Section 3 investigates the dynamical behavior of the proposed system, examining the influence of different parameters through techniques such as Lyapunov exponents spectrum, bifurcation diagrams, and phase plots. Furthermore, in Section 4, we propose a sliding mode control strategy for the new 4D CSCM, deriving the equivalent control law and validating its effectiveness through simulation studies. This study is summarized and concluding remarks are presented in the final section.

2. New 4D Chaotic Supply Chain Model (4D CSCM)

Supply chains are complex systems involving multiple interconnected components such as suppliers, manufacturers, distributors, retailers, and customers [29]. These components interact dynamically, with various factors influencing the overall performance and stability of the supply chain [30]. Traditional models have often been inadequate in capturing the inherent nonlinearities and chaotic behavior present in real-world supply chains. To address this, recent studies have focused on developing models that can better represent these complexities. One such model is the four-dimensional (4D) chaotic supply chain model, which extends the conventional three-dimensional models by incorporating an additional dimension.

Cuong et al. [31] described a four-tier integrated chaotic supply chain model, which can be represented by a system of differential equations. This model considers the interactions between product demand at a retailer, the quantity of product supplied by the distributor, the product produced by the manufacturer, and the product received by the customer. By incorporating various risk factors such as transportation risk, quality risk, distortion, contingency reserves, and safety stock, the model aims to provide a more realistic representation of supply chain dynamics. The four-tier integrated chaotic supply chain model uses the following 4D system of differential equations:

$$\begin{cases} \dot{x} = ay - (m + 1)x + dw \\ \dot{y} = cx - xz - y \\ \dot{z} = xy - bz \\ \dot{w} = -x - (m + 1)w \end{cases} \quad (1)$$

where x is product demand at a retailer, y is the quantity of product that the distributor can supply, z is the product produced at a manufacturer, and w is the product received by the customer. Moreover, in the chaotic supply chain model (1), we include various coefficients such that of transport risk a , quality risk b , distortion c , contingency reserve d , and safety stock m between customer and retailer.

When $a = m + 1$, the chaotic supply chain System (1) reduces to the 4D Lorenz–Stenflo system given by the dynamics

$$\begin{cases} \dot{x} = a(y - x) + dw \\ \dot{y} = cx - xz - y \\ \dot{z} = xy - bz \\ \dot{w} = -x - aw \end{cases} \quad (2)$$

When $a = 2, b = 1.05, c = 26$, and $d = 1.5$, a chaotic attractor is exhibited by the 4D CSCM (2) for the initial values $x(0) = y(0) = z(0) = w(0) = 0.04$. In fact, for $T = 1 \times 10^4$ s, the Lyapunov exponents for the Cuong System (2) were found to be:

$$L_1 = 0.4228, L_2 = 0, L_3 = -2.9262, L_4 = -3.5468 \quad (3)$$

This paper proposes a new chaotic supply chain system by adding a quadratic nonlinear term px^2 in the third differential equation of the Cuong chaotic System (2). Thus, our new 4D chaotic supply chain system can be modelled according to a system of differential equations:

$$\begin{cases} \dot{x} = a(y - x) + dw \\ \dot{y} = cx - xz - y \\ \dot{z} = xy - bz + px^2 \\ \dot{w} = -x - aw \end{cases} \quad (4)$$

We take new values for the system parameters as $a = 5.5, b = 1.8, c = 27, d = 1.6,$ and $p = 0.5$. We take the initial values of the System (4) as $x(0) = 0.04, y(0) = 0.04, z(0) = 0.04,$ and $w(0) = 0.04$. For $T = 1 \times 10^4$ s, we calculated the Lyapunov exponents for the new 4D System (4) and obtained the following:

$$L_1 = 0.8006, L_2 = 0, L_3 = -5.8404, L_4 = -8.7601. \quad (5)$$

We notice the positive Lyapunov exponent of the new chaotic supply chain System (4) is significantly greater than that of Cuong chaotic System (2). This implies that the new 4D CSCM (4) exhibits more complexity than the Cuong chaotic System (2). The phase portrait of the new 4D CSCM (4) can be seen in Figure 1.

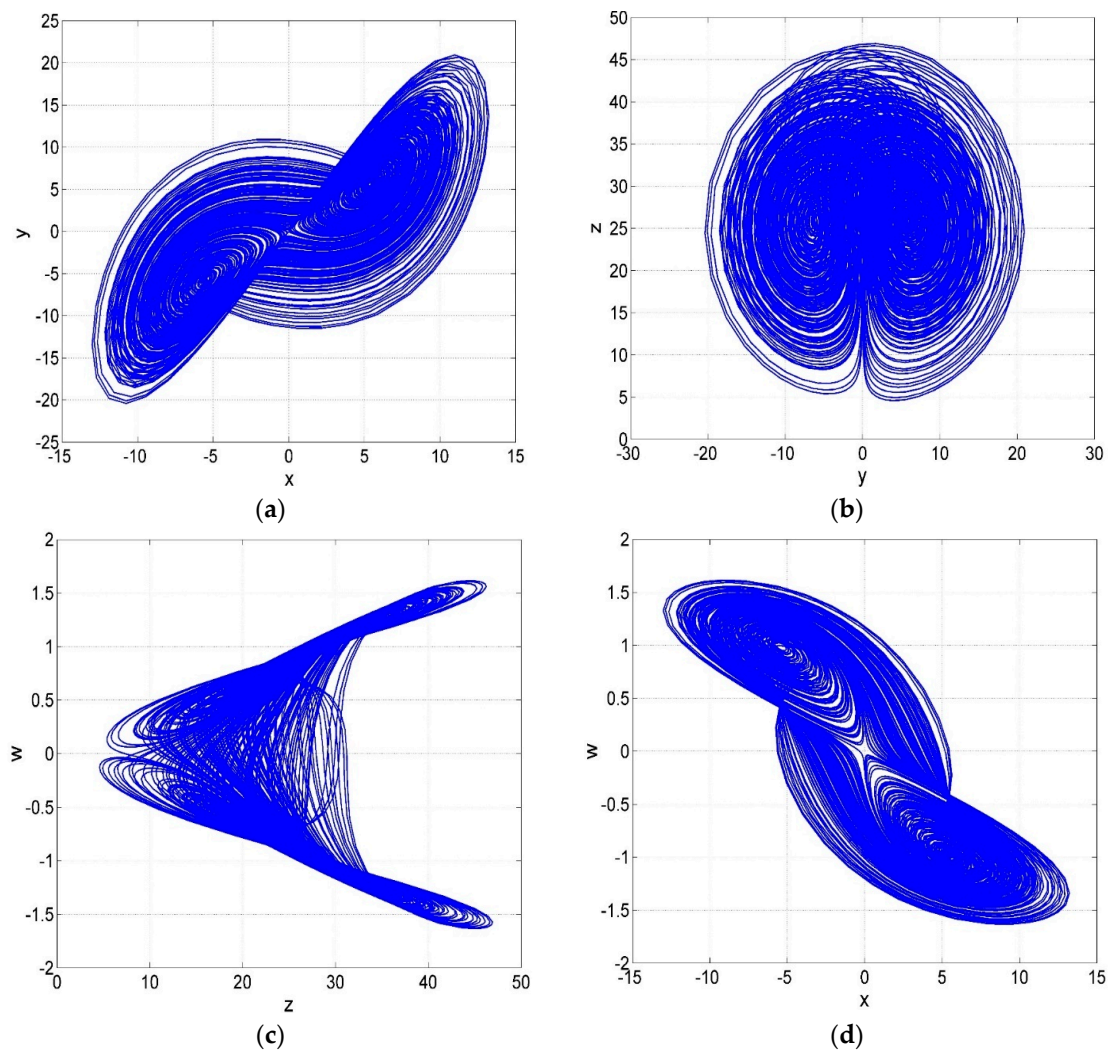


Figure 1. MATLAB simulation for System (4): (a) x-y plane, (b) y-z plane, (c) z-w plane, and (d) x-w plane.

3. Dynamical Analysis

In this section, we present a detailed examination of how the proposed system behaves, looking closely at how its parameters and initial conditions interact. Using various crucial techniques like Lyapunov exponents spectrum, bifurcation diagrams, and phase plots, we uncover how the system behaves, pinpointing areas of chaos, multistability, and other interesting phenomena. As explained further, our analysis reveals that the system is capable of producing chaotic behavior, with a maximum Lyapunov exponent of 1.48. Additionally, we discover the occurrence of multistability, providing a clear picture of its effects.

3.1. Influence of Parameter “a” on System’s Behavior

This subsection investigates the influence of parameter ‘a’ in shaping the behavior of the proposed system. By systematically varying parameter ‘a’ within the range of [5, 20], we explore its impact on the system’s dynamics. Through the bifurcation diagram and Lyapunov exponents spectrum shown in Figures 2a and 2b, respectively, we demonstrate that System (4) can exhibit chaotic and periodic behaviors for specific intervals of parameter ‘a’.

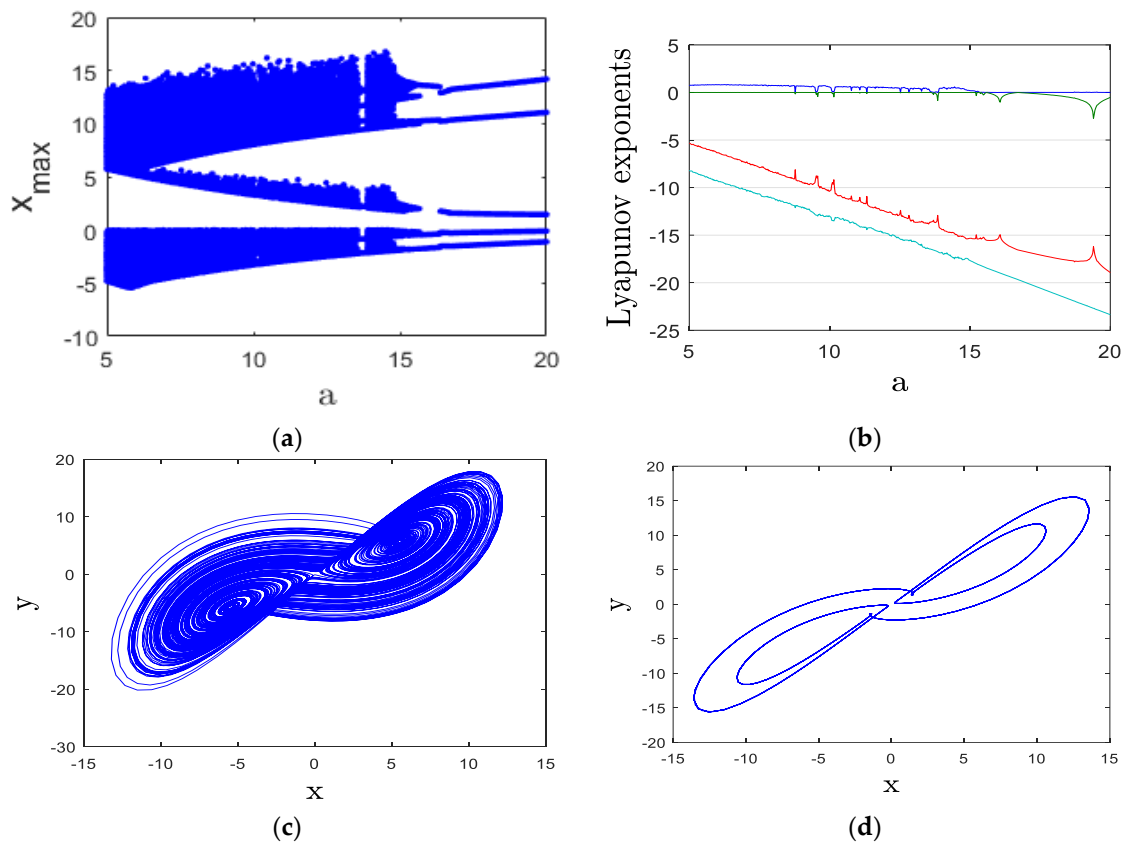


Figure 2. Chaotic exhibition of System (4): (a) bifurcation diagram, (b) Lyapunov exponents, (c) x-y chaotic attractor for a = 6, (d) x-y periodic attractor for a = 18.

When $5 < a < 15.3$, System (4) exhibits chaotic behavior, as demonstrated by Figure 2a. Additionally, Figure 2b clearly illustrates that the maximum Lyapunov exponent (MLE) is positive within this range. Furthermore, we observe windows of periodic behaviors nestled between chaotic regions at specific values of ‘a,’ namely, ([9.5, 9.6], [10.1, 10.15], [11.31, 11.34], [13.6, 13.9]). For enhanced clarity, we provide a visualization of the chaotic attractor in Figure 2c for the case when a = 6. The resulting Lyapunov exponents according to this setting are as follows: $LE1 = 0.812$, $LE2 = 0$, $LE3 = -6.338$, and $LE4 = -9.275$.

When $15.3 < a < 20$, System (4) demonstrates periodic behavior, as illustrated in Figure 2a. Furthermore, Figure 2b highlights that the maximum Lyapunov exponent (MLE) is zero within this interval. Additionally, for further insight, we present a visualization of the periodic attractor in Figure 2d corresponding to the case when $a = 18$. The resulting Lyapunov exponents according to this setting are as follows: $LE1 = 0$, $LE2 = -0.293$, $LE3 = -17.386$, and $LE4 = -21.123$.

Transportation risk is a significant factor in supply chain management, influencing the stability and performance of the entire system [32]. By varying the transportation risk parameter in our 4D CSCM, chaotic behavior in the supply chain due to transportation risk can be identified by irregular and unpredictable fluctuations in inventory levels, order quantities, and delivery schedules. This erratic behavior is often caused by factors such as delays, disruptions, and variability in transportation times. Periodic behavior, on the other hand, is characterized by regular, repeating patterns in the supply chain dynamics. This occurs when the transportation risk is more predictable and stable, leading to consistent and cyclical patterns in inventory and order levels.

3.2. Influence of Parameter “b” on System’s Behavior

In this subsection, we explore the influence of parameter ‘b’ on the behavior of System (4) by systematically varying it within the range of $[0, 2]$. This observation was based on the dynamics of the bifurcation diagram and Lyapunov exponents spectrum.

For $0 < b < 0.51$, System (4) demonstrates periodic behavior, as depicted in Figure 3a. Notably, Figure 3b reveals that the maximum Lyapunov exponent (MLE) is zero within this range. Furthermore, we observe intervals of chaotic behavior amidst periodic regions at specific values of ‘b’, namely, $([0.03, 0.07], [0.1, 0.13], [0.18, 0.20], [0.22, 0.25])$. Figure 3c illustrates the periodic attractor for the case when $b = 0.3$. The resulting Lyapunov exponents according to this setting are as follows: $LE1 = 0$, $LE2 = -0.349$, $LE3 = -4.756$, and $LE4 = -7.201$.

For $0.51 < b < 2$, System (4) exhibits chaotic behavior, except for the intervals when $b = [0.71, 0.76]$, $b = 0.82$, and $b = 0.96$, where it demonstrates periodic behavior, as found in Figure 3a. Additionally, Figure 3b gives an indication of positive MLE within this range. To provide further insight, we present a visualization of the chaotic attractor in Figure 3d corresponding to the case when $b = 2$. The resulting Lyapunov exponents according to this setting are as follows: $LE1 = 0.789$, $LE2 = 0$, $LE3 = -5.814$, and $LE4 = -8.975$.

Chaotic behavior due to quality risk is characterized by unpredictable fluctuations in product quality, leading to erratic order quantities, inventory levels, and customer satisfaction [33]. Factors contributing to chaotic behavior include inconsistent production processes, supplier quality issues, and variable inspection standards. In the chaotic regime, phase portraits of supply chain variables (e.g., product quality vs. inventory level) show intricate, non-repeating patterns, indicating high sensitivity to initial conditions. Small changes in quality risk can lead to significantly different outcomes, highlighting the unpredictable nature of the system. Periodic behavior, in contrast, is characterized by regular, repeating patterns in the supply chain dynamics due to stable and predictable product quality. This occurs when quality risk is minimized through consistent production processes and reliable suppliers. In the periodic regime, phase portraits show closed, repeating loops, indicating stable and predictable behavior. Periodic behavior allows for consistent product quality, enhancing customer satisfaction and reducing the need for returns or rework.

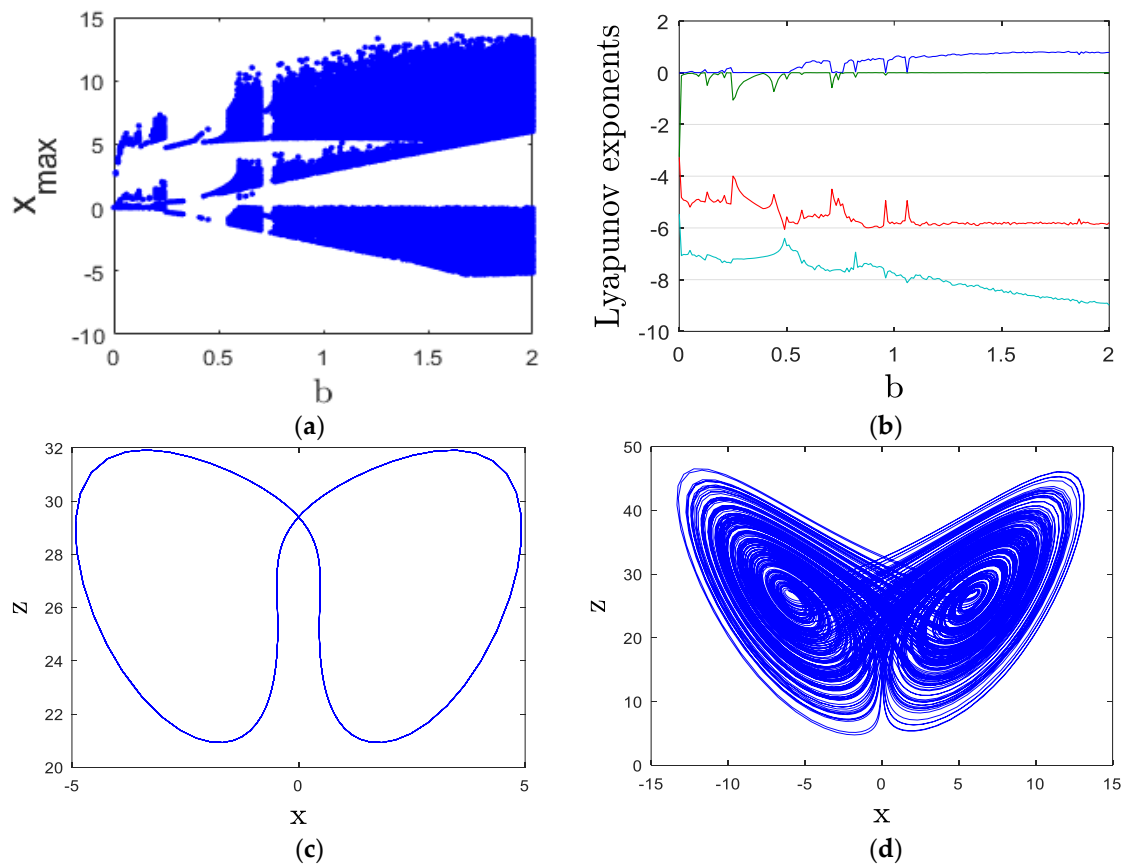


Figure 3. Chaotic exhibition of System (4): (a) bifurcation diagram, (b) Lyapunov exponents, (c) x-z periodic attractor for $b = 0.3$, (d) x-z chaotic attractor for $b = 2$.

3.3. Influence of Parameter “c” on System’s Behavior

This subsection examines the effect of systematically varying parameter ‘c’ on the system’s behavior within the range of [20, 200]. This observation was drawn from the dynamics of the bifurcation diagram and Lyapunov exponents spectrum.

For the interval of c ([20, 82], [90, 145.5]), System (4) displays chaotic behavior, with exceptions noted when $c = [57, 57.5]$, $c = 49.5$, $c = 197$, $c = 138.5$, and $c = 141.5$, where it exhibits periodic behavior, as shown in Figure 4a. Moreover, Figure 4b indicates a positive maximum Lyapunov exponent (MLE) within this range. To offer deeper insight, we provide a visualization of the chaotic attractor in Figure 4c corresponding to the case when $c = 110$. The resulting Lyapunov exponents according to this setting are as follows: $LE1 = 1.482$, $LE2 = 0$, $LE3 = -5.572$, and $LE4 = -9.710$.

For the range of c ([92, 90], [145.5, 200]), System (4) demonstrates periodic behavior, as illustrated in Figure 4a. Notably, Figure 4b reveals that the MLE is zero within this interval. Figure 4d illustrates the periodic attractor for the case when $c = 89$. The resulting Lyapunov exponents according to this setting are as follows: $LE1 = 0$, $LE2 = -2.591$, $LE3 = -2.849$, and $LE4 = -8.373$.

Distortion in supply chain management refers to discrepancies and inaccuracies in information flow, demand forecasts, and order quantities, often leading to the well-known “bullwhip effect” [34,35]. In the chaotic regime, phase portraits of supply chain variables (e.g., order quantity vs. inventory level) show complex, non-repeating patterns, indicating high sensitivity to initial conditions. Small changes in distortion can lead to significantly different outcomes, highlighting the unpredictable nature of the system. Periodic behavior, in contrast, is characterized by regular, repeating patterns in the supply chain dynamics due to accurate and timely information flow. This occurs when distortion is minimized through synchronized communication and reliable data analytics.

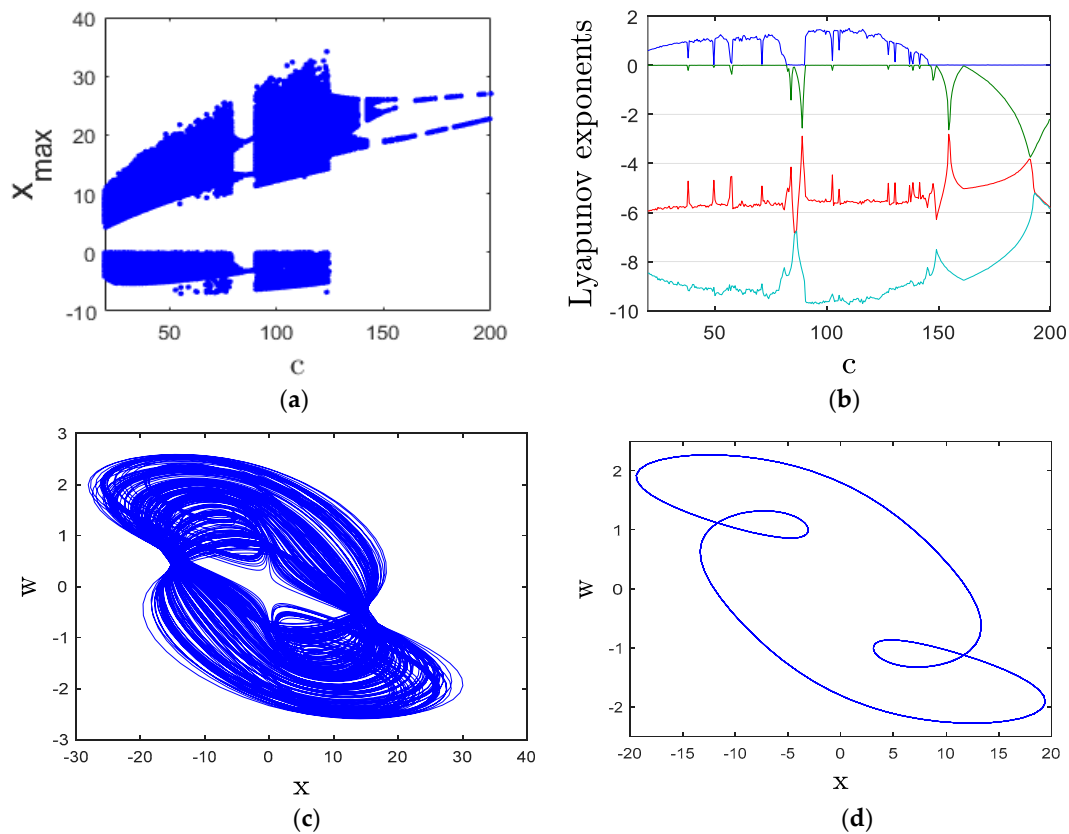


Figure 4. Chaotic exhibition of System (4): (a) bifurcation diagram, (b) Lyapunov exponents, (c) x-w chaotic attractor for $c = 110$, (d) x-w periodic attractor for $c = 89$.

3.4. Influence of Parameter “d” on System’s Behavior

In this subsection, we explore the impact of parameter ‘d’ on the system’s behavior by systematically varying it within the range of $[-35, 5]$. This observation was drawn from the dynamics of the bifurcation diagram and Lyapunov exponents spectrum.

For the interval of d $([-35, -25.5], [-22.8, -20.2])$, System (4) predominantly exhibits periodic behavior, except for the subrange of d $[-20.7, -20.45]$, where chaos emerges, as found in Figure 5a. Notably, Figure 5b suggests a zero maximum Lyapunov exponent (MLE) within this interval. Figure 5c illustrates the periodic attractor for the case when $d = -27$. The resulting Lyapunov exponents according to this setting are as follows: $LE1 = 0$, $LE2 = -0.468$, $LE3 = -0.499$, and $LE4 = -12.841$.

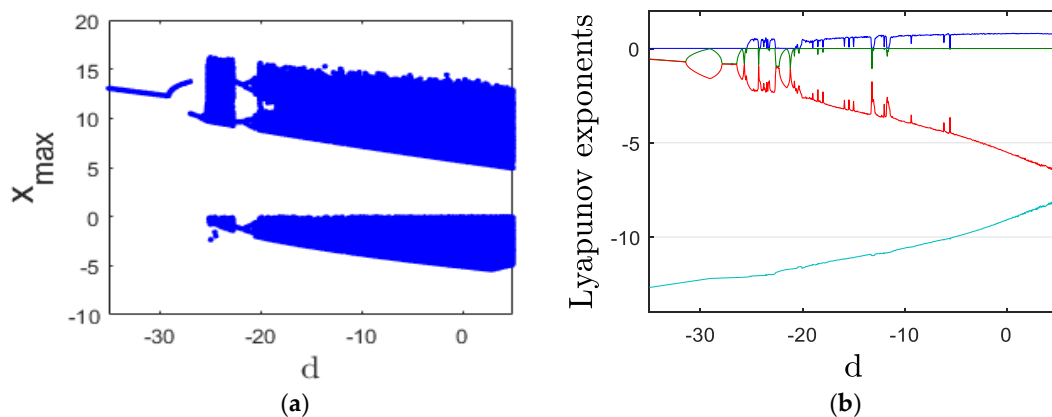


Figure 5. Cont.

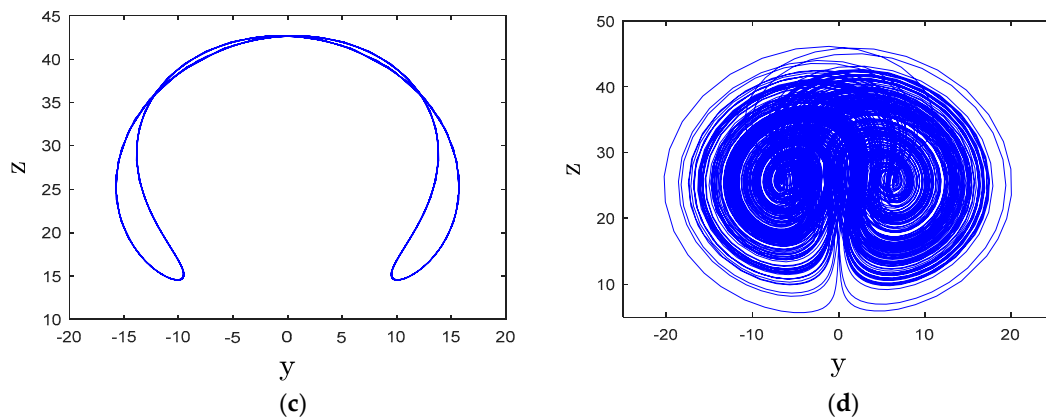


Figure 5. Chaotic exhibition of System (4): (a) bifurcation diagram, (b) Lyapunov exponents, (c) y-z periodic attractor for $d = -27$, (d) y-z chaotic attractor for $d = 1$.

Within the range of d ($[-25.5, -22.8]$, $[-20.2, 5]$), System (4) predominantly displays chaotic behavior. However, exceptions occur at specific values such as $d = [(-24.3, -24.15), (-23.35, -23.25), (-13.25, -13), (-11.75, -11.55)]$, $d = -18.5$, and $d = -18$, where periodic behavior is observed, as depicted in Figure 5a. Additionally, Figure 5b highlights a positive maximum Lyapunov exponent (MLE) within this range. To provide further insight, we present a visualization of the chaotic attractor in Figure 5d corresponding to the case when $d = 1$. The resulting Lyapunov exponents according to this setting are as follows: $LE1 = 0.772$, $LE2 = 0$, $LE3 = -5.669$, and $LE4 = -8.903$.

Contingency reserves in supply chain management refer to the additional inventory or resources kept to buffer against uncertainties and disruptions [36]. Chaotic behavior due to poorly managed contingency reserves is characterized by erratic and unpredictable fluctuations in inventory levels, leading to inefficiencies and instability in the supply chain. In the chaotic regime, phase portraits of supply chain variables (e.g., inventory level vs. order quantity) show intricate, non-repeating patterns, indicating high sensitivity to initial conditions. Periodic behavior, in contrast, is characterized by regular, repeating patterns in the supply chain dynamics due to well-managed contingency reserves. This occurs when contingency reserves are appropriately sized and consistently utilized to buffer against demand variability and disruptions.

3.5. Influence of Parameter “p” on System’s Behavior

In this subsection, we explore the impact of parameter ‘p’ on the system’s behavior by systematically varying it within the range of $[0.5, 10]$. This observation was drawn from the dynamics of the bifurcation diagram and Lyapunov exponents spectrum.

When choosing p between $([0.5, 9.3])$, we observe a clear sign of chaotic behavior in System (4), as found in Figure 6a. Furthermore, Figure 6b indicates a positive maximum Lyapunov exponent (MLE) within this range. To provide a deeper understanding, we present a visualization of the chaotic attractor in Figure 6c corresponding to the scenario when $p = 3$. The resulting Lyapunov exponents according to this setting are as follows: $LE1 = 1.022$, $LE2 = 0$, $LE3 = -5.601$, and $LE4 = -9.222$.

For the range of p $[9.3, 10]$, System (4) demonstrates periodic behavior, except for instances when p is in the intervals $[9.94, 10]$, $p = 9.35$, and $p = 9.5$, as illustrated in Figure 6a. Notably, Figure 6b reveals that the MLE is zero within this interval. Figure 6d illustrates the periodic attractor for the scenario when $p = 9.8$. The resulting Lyapunov exponents according to this setting are as follows: $LE1 = 0$, $LE2 = -0.777$, $LE3 = -3.791$, and $LE4 = -9.238$.

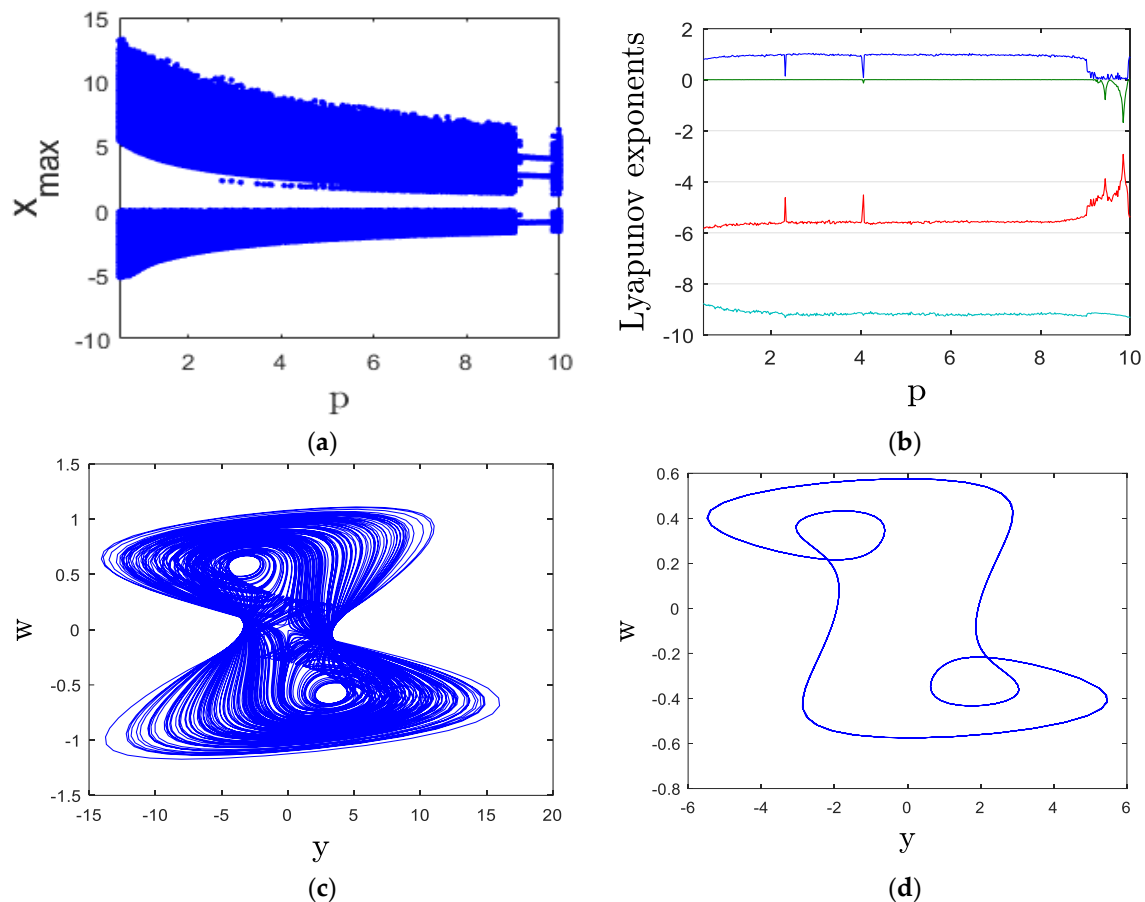


Figure 6. Chaotic exhibition of System (4): (a) bifurcation diagram, (b) Lyapunov exponents, (c) y - w chaotic attractor for $p = 3$, (d) y - w periodic attractor for $p = 9.8$.

Chaotic behavior due to improperly managed safety stock is characterized by irregular and unpredictable fluctuations in inventory levels, leading to instability in the supply chain [37]. Factors contributing to chaotic behavior include inappropriate sizing of safety stock and inconsistent replenishment policies. Chaotic behavior due to safety stock can lead to frequent overstocking or stockouts, increasing holding costs and reducing service levels. Also, periodic behavior allows for consistent service levels and efficient inventory management, reducing the likelihood of stockouts and excess inventory.

3.6. Influence of Initial Conditions on System's Behavior

In this section, we explore how the choice of initial conditions potentially affects the behavior of the system we have proposed. We discuss its multistability and the coexistence of different chaotic attractors by considering fixed parameter values yet with different initial points [38–41]. To demonstrate this interesting phenomenon, we choose two distinct initial points: $[0.04 \ 0.04 \ 0.04 \ 0.04]$, shown in blue, and $[-0.04 \ 0.04 \ 0.04 \ 0.04]$, shown in red. Next, we create a bifurcation diagram for System (4) with c values ranging from 130 to 200. The resulting diagram, displayed in Figure 7a, clearly shows the presence of multistability in the system.

In Figure 7b–d, you can see three pairs of coexisting chaotic attractors generated by System (4) for $c = 135$, $c = 140$, and $c = 145$, respectively. Figure 7e,f depict two pairs of coexisting periodic attractors for $c = 147$ and $c = 190$, respectively. The existence of coexisting distinct attractors under identical parameter settings underscores the complex dynamical nature of the proposed system, offering valuable insights into its behavior and potential applications.

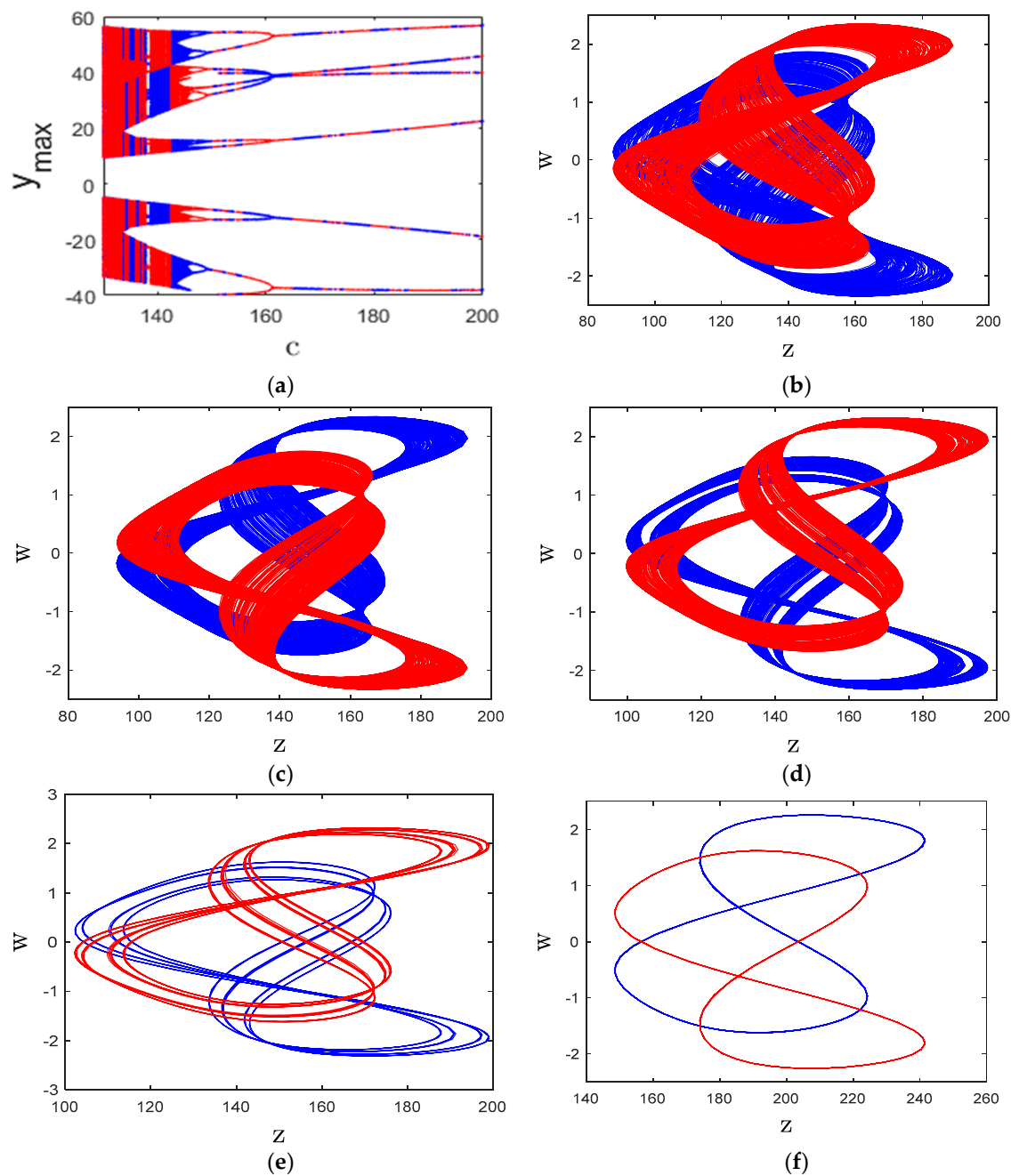


Figure 7. Chaotic exhibition of System (4): (a) bifurcation diagram, (b) two coexisting chaotic attractors for $c = 135$, (c) two coexisting chaotic attractors for $c = 140$, (d) two coexisting chaotic attractors for $c = 145$, (e) two coexisting periodic attractors for $c = 147$, (f) two coexisting periodic attractors for $c = 190$.

4. Sliding Mode Controller

Traditionally, two main steps are considered in the design of sliding model control. The first step is the selection of the sliding surface and the second step is the control law to stay on the sliding surface [42,43]. In practice and computer implementations, other steps must be considered. Therefore, in this article, all the steps of designing the sliding model controller will be described. Initially, with initial conditions, the system will have an output. This output will be compared with the desired values and the error will be obtained. The error block has two outputs, the first is the error and the second is its derivative.

In the next block, the sliding method calculates the sliding surface and its derivative using the error and the derivative of the error (of course, the sliding surface is selected by the designer, but finally the slip surface and the derivative of the sliding surface must be calculated). The equivalent control law is obtained from the two parameters of the sliding surface and the derivative of the sliding surface. This control law is called equivalent controller. In the design of the sliding mode controller, the exponential reaching law is added to the equivalent controller. Finally, the sliding model controller will be activated. This cycle continues until the output of the system tends to the desired values. The block diagram in Figure 8 depicts this cycle.

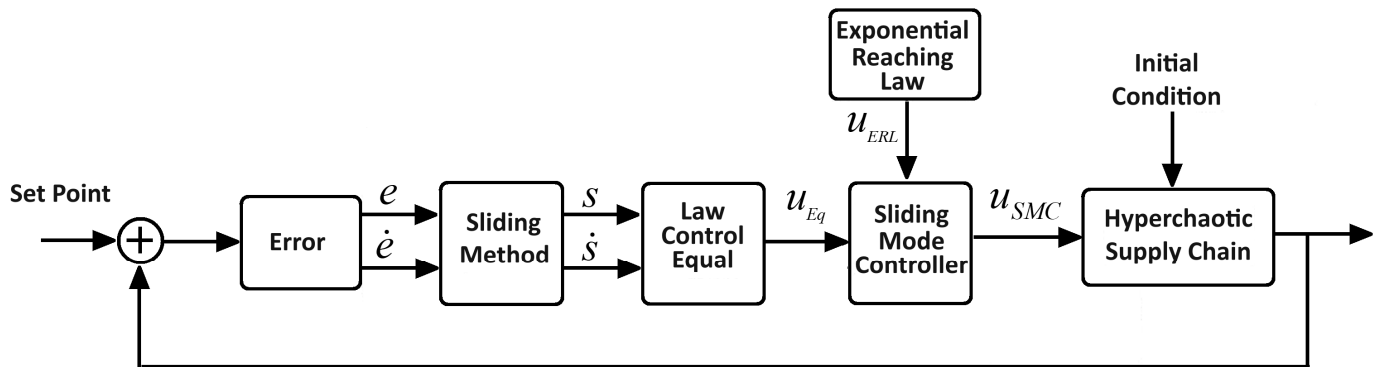


Figure 8. Block diagram of the design steps of the sliding model controller.

In this paper, the main goal was to eliminate the chaotic behavior in the 4D chaotic supply chain.

So, Equation (6) was rewritten as follows:

$$\begin{cases} \dot{x} = a(y - x) + dw + u_{SMC_x} \\ \dot{y} = cx - xz - y + u_{SMC_y} \\ \dot{z} = xy - bz + px^2 + u_{SMC_z} \\ \dot{w} = -x - aw + u_{SMC_w} \end{cases} \quad (6)$$

where u_{SMC_x} , u_{SMC_y} , u_{SMC_z} , u_{SMC_w} are the proposed sliding model controllers and should be designed.

Step 1: The first step is to calculate the error. The error function is defined as follows:

$$\begin{cases} e_x = x - x^* \\ e_y = y - y^* \\ e_z = z - z^* \\ e_w = w - w^* \end{cases} \quad (7)$$

where x^* , y^* , z^* , w^* are the desired values (set point) to reach our control goal.

Step 2: Calculation of the error derivative, according to Equation (7), so:

$$\begin{cases} \dot{e}_x = \dot{x} - \dot{x}^* \\ \dot{e}_y = \dot{y} - \dot{y}^* \\ \dot{e}_z = \dot{z} - \dot{z}^* \\ \dot{e}_w = \dot{w} - \dot{w}^* \end{cases} \quad (8)$$

Step 3: The selection of the sliding surface is very important in the design problem of the sliding model controller. Therefore, the sliding surface in this design is considered as follows:

$$\begin{cases} s_x = e_x(t) + \int_0^t \zeta_x e_x(\tau) d\tau \\ s_y = e_y(t) + \int_0^t \zeta_y e_y(\tau) d\tau \\ s_z = e_z(t) + \int_0^t \zeta_z e_z(\tau) d\tau \\ s_w = e_w(t) + \int_0^t \zeta_w e_w(\tau) d\tau \end{cases} \tag{9}$$

where $\zeta_x, \zeta_y, \zeta_z, \zeta_w$ are constant values.

Step 4: To determine the derivative of the sliding surface, the derivative is taken from Equation (9):

$$\begin{cases} \dot{s}_x = \dot{e}_x(t) + \zeta_x e_x(t) \\ \dot{s}_y = \dot{e}_y(t) + \zeta_y e_y(t) \\ \dot{s}_z = \dot{e}_z(t) + \zeta_z e_z(t) \\ \dot{s}_w = \dot{e}_w(t) + \zeta_w e_w(t) \end{cases} \tag{10}$$

To reach the equivalent control law, the condition $s=0$ must be satisfied. Therefore:

$$\begin{cases} \dot{e}_x(t) + \zeta_x e_x(t) = 0 \\ \dot{e}_y(t) + \zeta_y e_y(t) = 0 \\ \dot{e}_z(t) + \zeta_z e_z(t) = 0 \\ \dot{e}_w(t) + \zeta_w e_w(t) = 0 \end{cases} \tag{11}$$

Step 5: Determine the equivalent controller. By replacing Equation (8) in Equation (11) and simplifying, the equivalent controller is obtained:

$$\begin{cases} u_{x_{eq}} = -a(y - x) - d w - x^* - \zeta_x e_x(t) \\ u_{y_{eq}} = -c x + x z + y - y^* - \zeta_y e_y(t) \\ u_{z_{eq}} = -x y + b z - p x^2 - z^* - \zeta_z e_z(t) \\ u_{w_{eq}} = x + a w - w^* - \zeta_w e_w(t) \end{cases} \tag{12}$$

where u are equivalent controllers. To achieve the final model sliding control, the exponential control law should also be added to the equivalent controller. So:

$$\begin{cases} u_{SMC_x} = u_{x_{eq}} + u_{x_{ERL}} \\ u_{SMC_y} = u_{y_{eq}} + u_{y_{ERL}} \\ u_{SMC_z} = u_{z_{eq}} + u_{z_{ERL}} \\ u_{SMC_w} = u_{w_{eq}} + u_{w_{ERL}} \end{cases} \tag{13}$$

Step 6: Obtain the exponential control law, which is the exponential control law in Equation (13) and is obtained from the following relationship.

$$\begin{cases} u_{x_{ERL}} = k_x s_x + \alpha_x \frac{s_x}{|s_x| + \epsilon_x} \\ u_{y_{ERL}} = k_y s_y + \alpha_y \frac{s_y}{|s_y| + \epsilon_y} \\ u_{z_{ERL}} = k_z s_z + \alpha_z \frac{s_z}{|s_z| + \epsilon_z} \\ u_{w_{ERL}} = k_w s_w + \alpha_w \frac{s_w}{|s_w| + \epsilon_w} \end{cases} \tag{14}$$

In the last equation, k, ϵ are the gains of the exponential control law. Of course, it is obvious that:

$$\lim_{\epsilon \rightarrow 0} \left(\alpha \frac{s}{|s| + \epsilon} \right) = \alpha \text{sign}(s) \tag{15}$$

Verification of the sliding model controller design is carried out with the help of Theorem 1.

Theorem 1. *The behavior of the chaotic equations of the supply chain (6) under the controller of the following proposed sliding model tends to the desired values when the initial condition values $x(0), y(0), z(0), w(0) \in \mathbb{R}$.*

$$\begin{cases} u_{SMC_x} = -a(y - x) - dw - x^* - \zeta_x e_x(t) + k_x s_x + \alpha_x \frac{s_x}{|s_x| + \epsilon_x} \\ u_{SMC_y} = -cx + xz + y - y^* - \zeta_y e_y(t) + k_y s_y + \alpha_y \frac{s_y}{|s_y| + \epsilon_y} \\ u_{SMC_z} = -xy + bz - px^2 - z^* - \zeta_z e_z(t) + k_z s_z + \alpha_z \frac{s_z}{|s_z| + \epsilon_z} \\ u_{SMC_w} = x + aw - w^* - \zeta_w e_w(t) + k_w s_w + \alpha_w \frac{s_w}{|s_w| + \epsilon_w} \end{cases} \tag{16}$$

Proof. Consider the candidate Lyapunov function as follows:

$$V(s) = \frac{1}{2}(s_x^2 + s_y^2 + s_z^2 + s_w^2) \tag{17}$$

If the Equation (17) is derived, then:

$$\dot{V}(s) = \dot{s}_x s_x + \dot{s}_y s_y + \dot{s}_z s_z + \dot{s}_w s_w \tag{18}$$

By inserting and simplifying Equation (18):

$$\begin{aligned} \dot{V}(s) &= s_x(\dot{e}_x(t) + \zeta_x e_x(t)) + s_y(\dot{e}_y(t) + \zeta_y e_y(t)) + \\ & \quad s_z(\dot{e}_y(t) + \zeta_y e_y(t)) + s_w(\dot{e}_w(t) + \zeta_w e_w(t)) \\ &\Rightarrow s_x(k_x s_x + \alpha_x \frac{s_x}{|s_x| + \epsilon_x}) + s_y(k_y s_y + \alpha_y \frac{s_y}{|s_y| + \epsilon_y}) + \\ & \quad s_z(k_z s_z + \alpha_z \frac{s_z}{|s_z| + \epsilon_z}) + s_w(k_w s_w + \alpha_w \frac{s_w}{|s_w| + \epsilon_w}) \end{aligned} \tag{19}$$

Equation (19) will always be negative ($\dot{V}(s) < 0$) if and only if $\alpha_{x,y,z,w}, k_{x,y,z,w} < 0$. \square

In the numerical simulation, MATLAB R2022a software was used to calculate the supply chain responses of Equation (6). The initial condition values were equal to $[x(0) \ y(0) \ z(0) \ w(0)]^T = [0.04 \ 0.04 \ 0.04 \ 0.04]$. The sliding mode controller parameters were equal to $\alpha_{x,y,z,w} = 0.01, k_{x,y,z,w} = -0.1$ and $\zeta_{x,y,z,w} = -2$ were also selected. The desired values in this part of the simulation were zero ($x^* = y^* = z^* = w^* = 0$). Figure 9 shows the new 4D chaotic supply chain under the proposed sliding model controller. The control strategy was activated from time $t = 4$.

Figure 10 depicts the behavior of the proposed sliding model controller. As can be seen from Figure 10, the controller reached zero value after a short time. Figure 11 shows that the sliding surface converged to zero exponentially over time.

In the other part of the simulation, the tracking of other desired values was investigated in Table 1. In this way, after reaching the first desired values, the second desired values were tracked.

Table 1. The different time sequences.

Seq.	Time	Desired Value	Sliding Mode
1	$0 < \text{Time} < 4$	none	off
2	$4 < \text{Time} < 10$	$x^* = y^* = z^* = w^* = 0$	on
3	$10 < \text{Time} < \infty$	$x^* = y^* = z^* = w^* = 5$	on

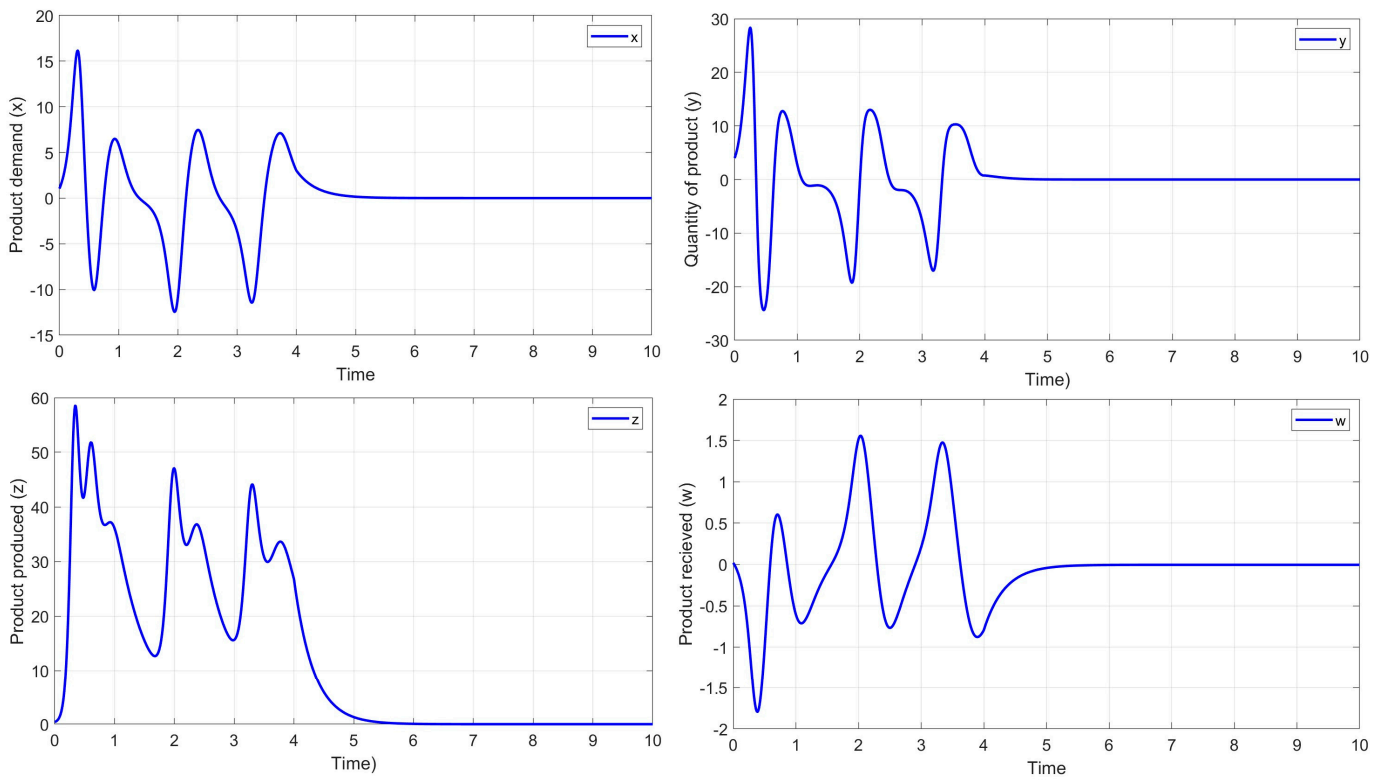


Figure 9. Elimination of chaotic behavior in 4D supply chain with the proposed sliding model control method.

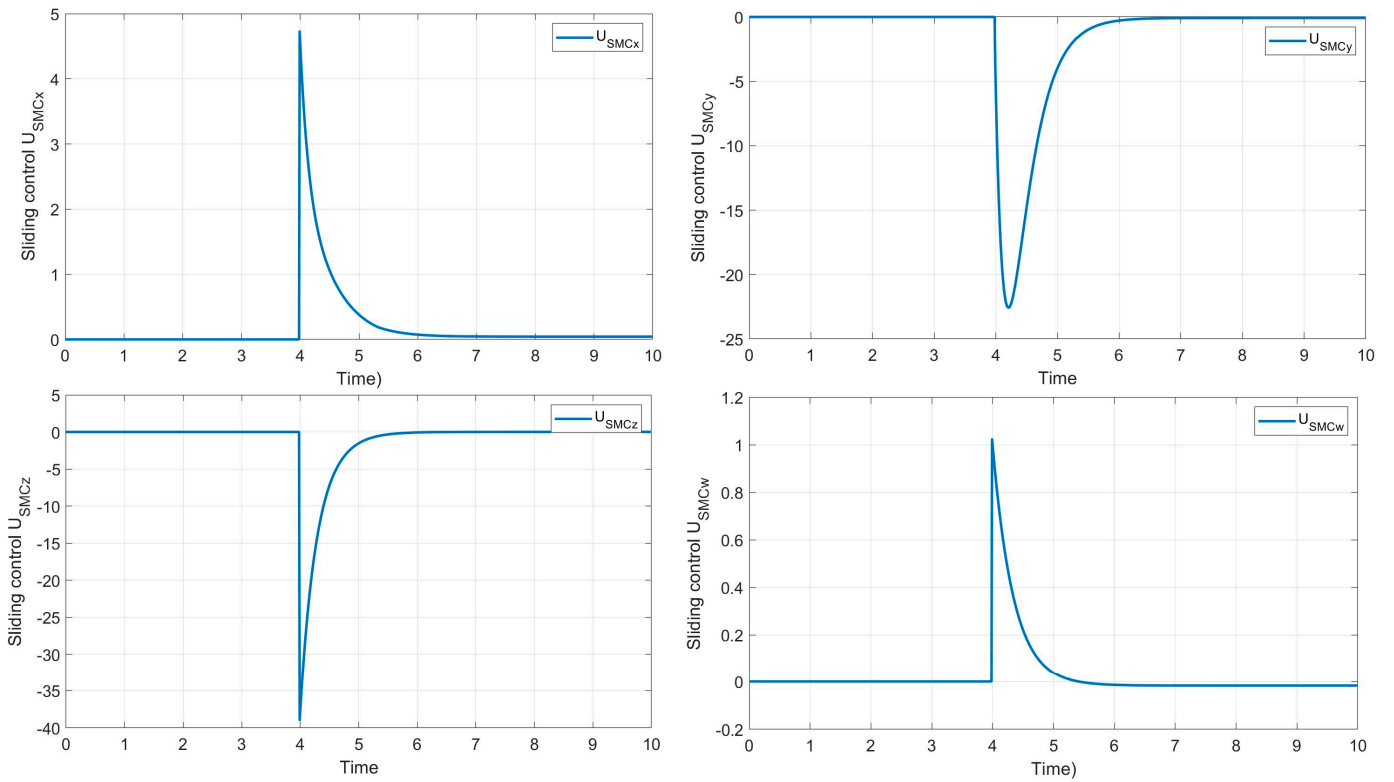


Figure 10. Behavior of the proposed sliding model controller.

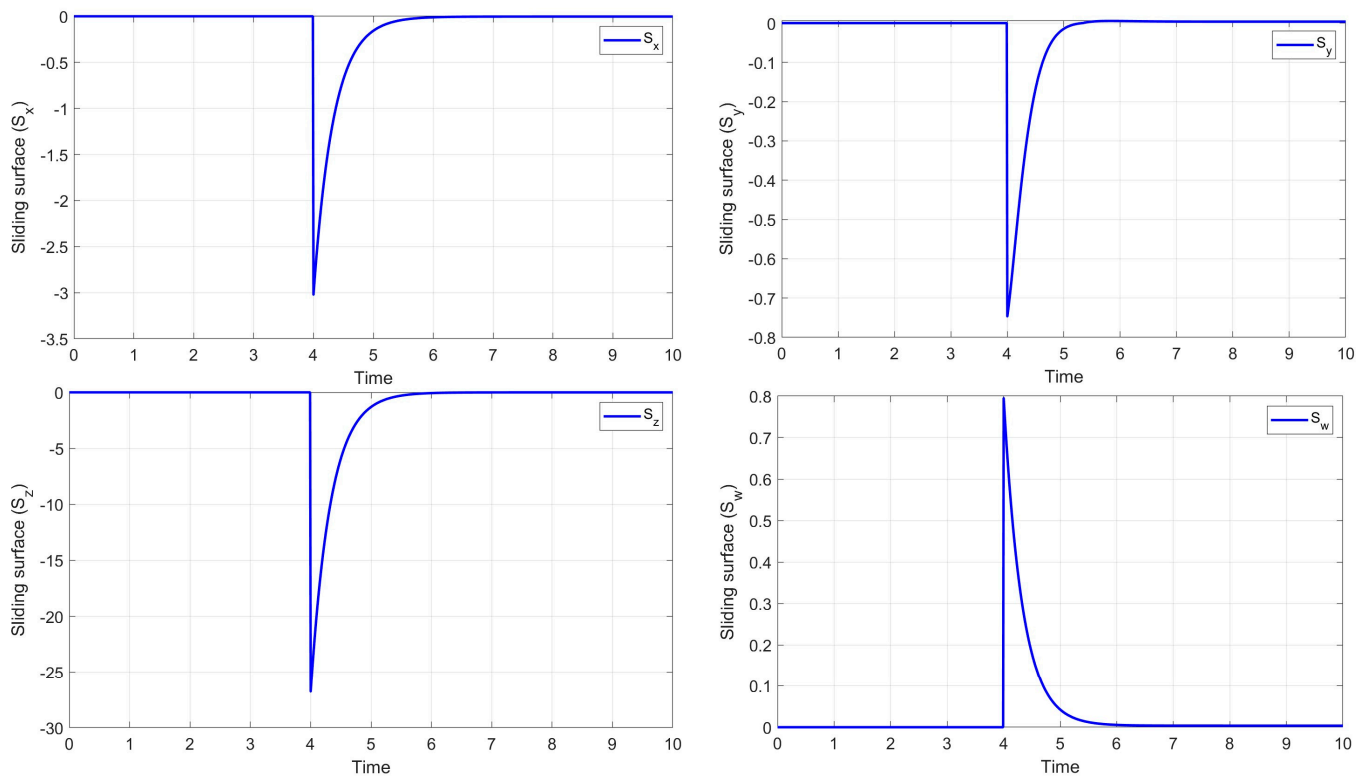


Figure 11. The behavior of the sliding surface.

When physical systems are involved in chaos, they cause great damage to organizations and systems in the real world. Therefore, controller design methods should be able to remove chaotic behavior from the system in a short period of time and also track it if desired values are required. Therefore, the time to reach stability is defined from the time the controller is applied until the zero error is reached. Figure 12 show the chaos removal and optimal value tracking under the proposed sliding model controller and Figure 13 show the behavior of the sliding model controller in order to track the desired values after removing the chaos. In the sliding model controller design method, the time to reach stability and eliminate chaos is approximately equal to $t = 1.8$. This value can be controlled by setting the parameters $\zeta_x, \zeta_y, \zeta_z, \zeta_w$ in Equation (9). Figure 14 shows the comparison of chaotic supply chain behavior with changing values $\zeta_x, \zeta_y, \zeta_z, \zeta_w$, and Figure 15 shows the behavior of the proposed sliding model controller with different $\zeta_x, \zeta_y, \zeta_z, \zeta_w$ values.

As can be seen, the more negative zeta values increase the speed of convergence towards the desired values. But the important point is the controller’s behavioral conditions, which have sharp points and more magnitude. Controller behavior can represent real-world implementation cost. In other words, in physical systems, the control signal is applied to the actuator, but if this signal has high frequencies, the actuator may not be able to respond to it. In supply chain systems, the control signal is the same as management decisions. Also, the actuator in supply chain systems is interpreted as organizational agility. Therefore, if an organization is agile and fast, it can respond to quick management decisions. Otherwise, in physical systems or supply chain systems, the fast behavior of the controller is not seen by the driver.

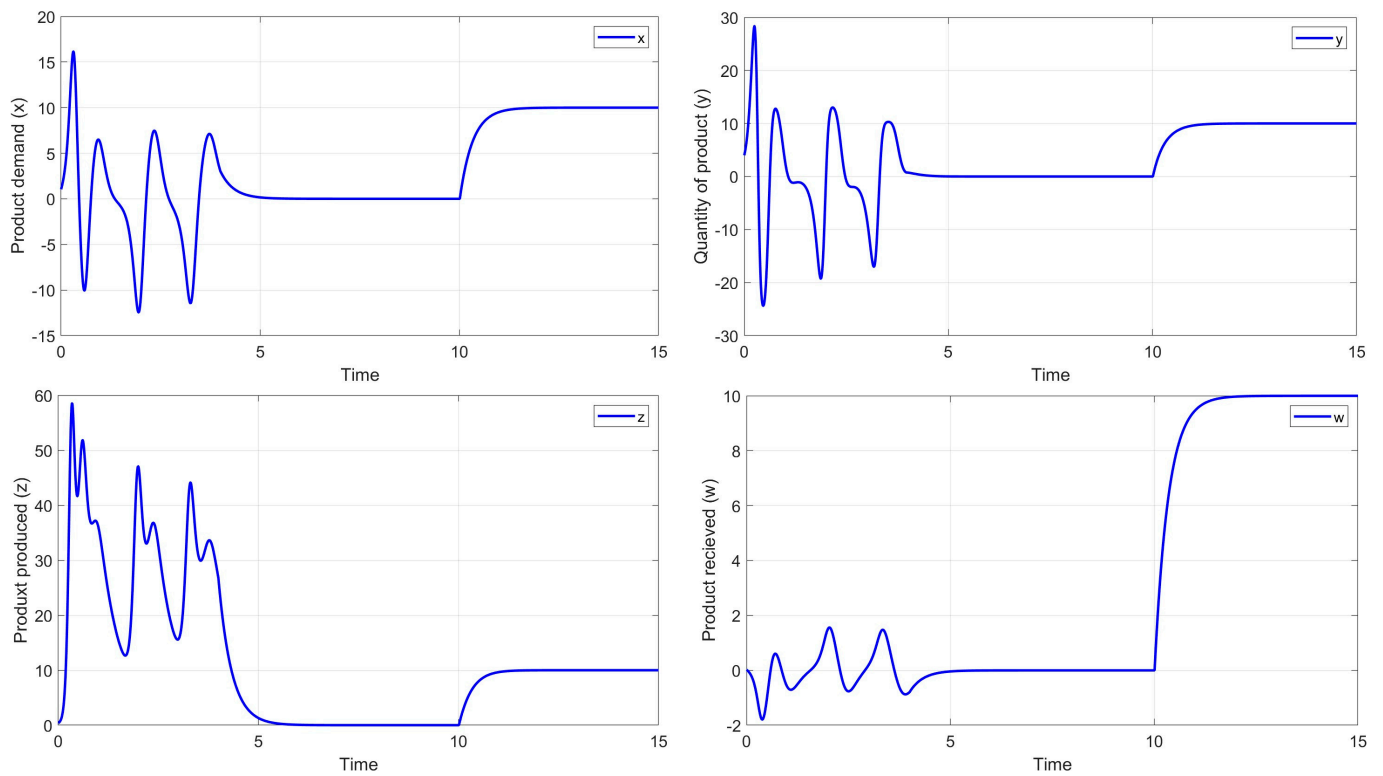


Figure 12. Chaos removal and optimal value tracking under the proposed sliding model controller.

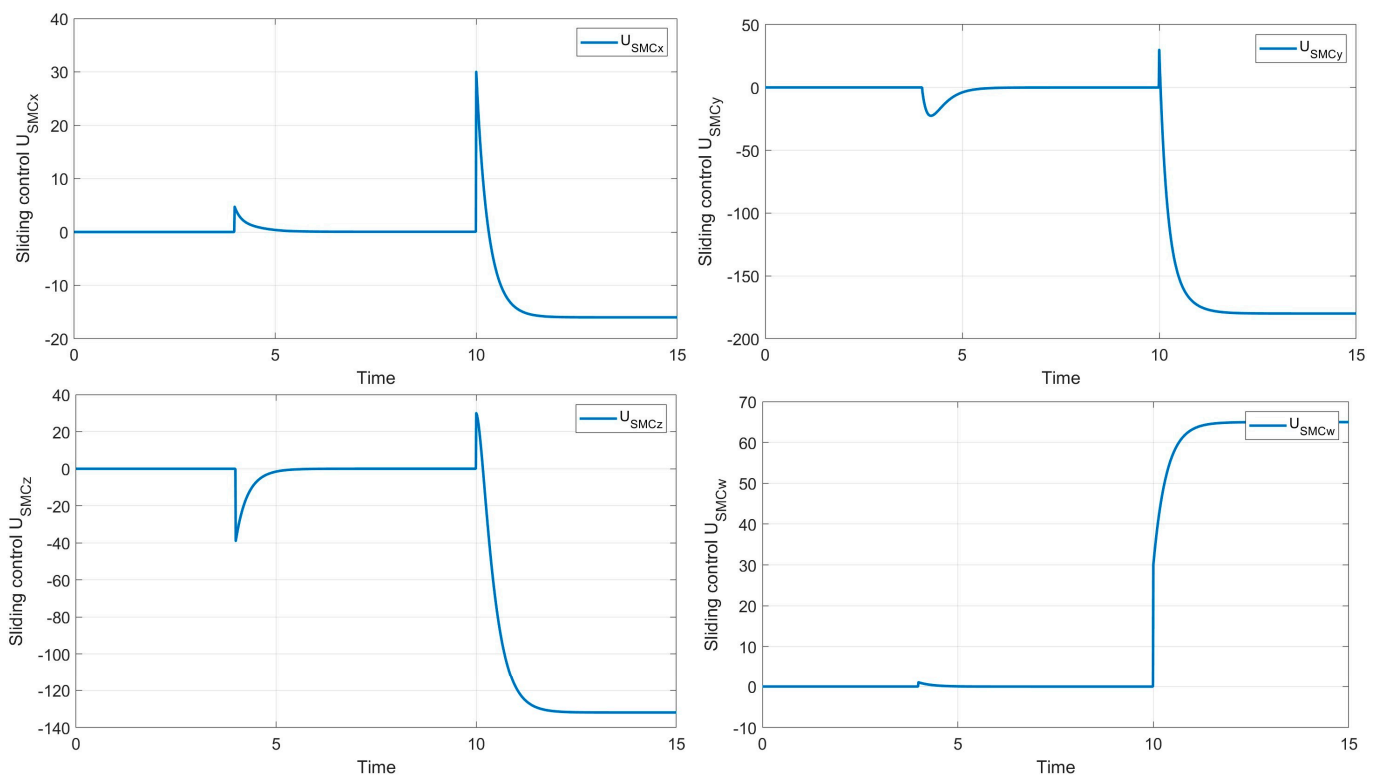


Figure 13. The behavior of the sliding model controller in order to track the desired values after removing the chaos.

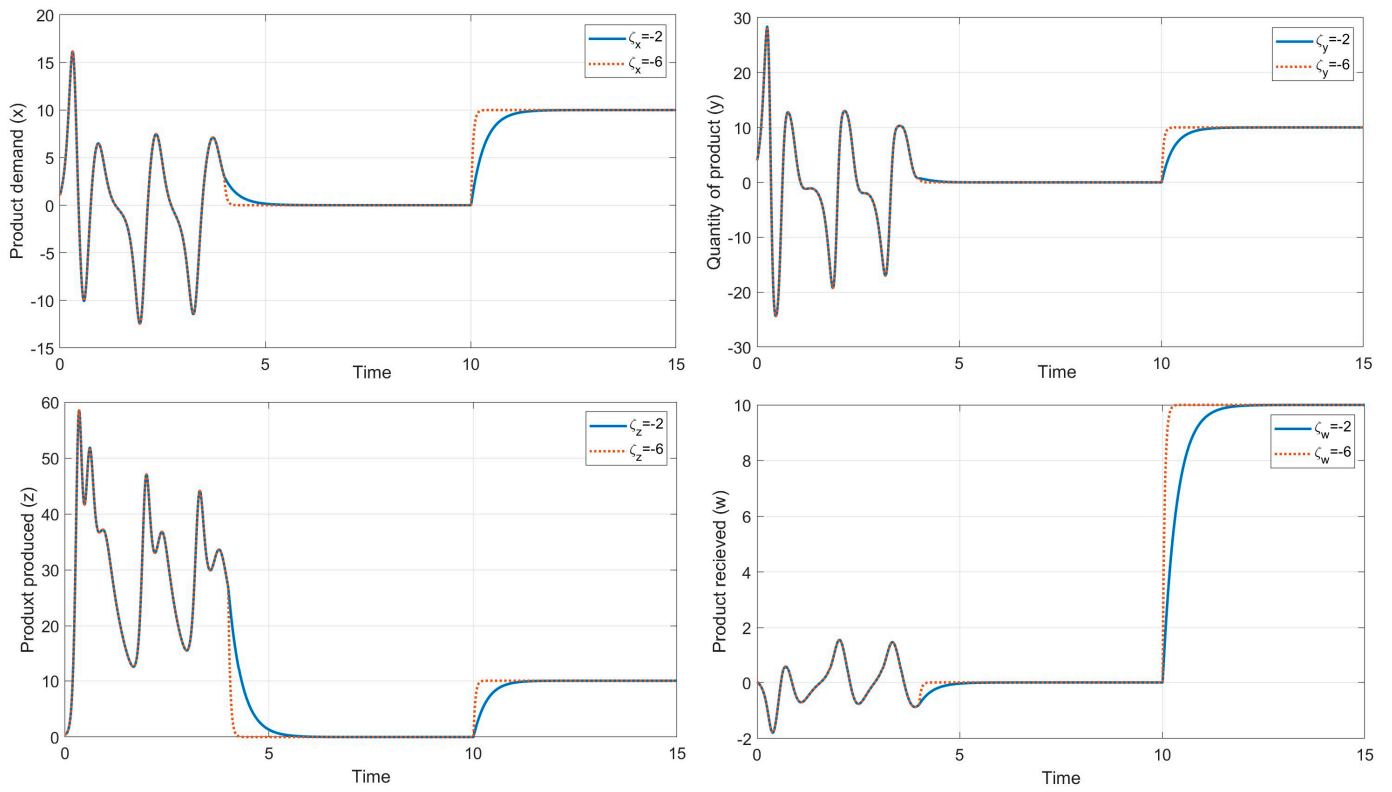


Figure 14. Chaotic supply chain behavior with changing values $\zeta_x, \zeta_y, \zeta_z, \zeta_w$.

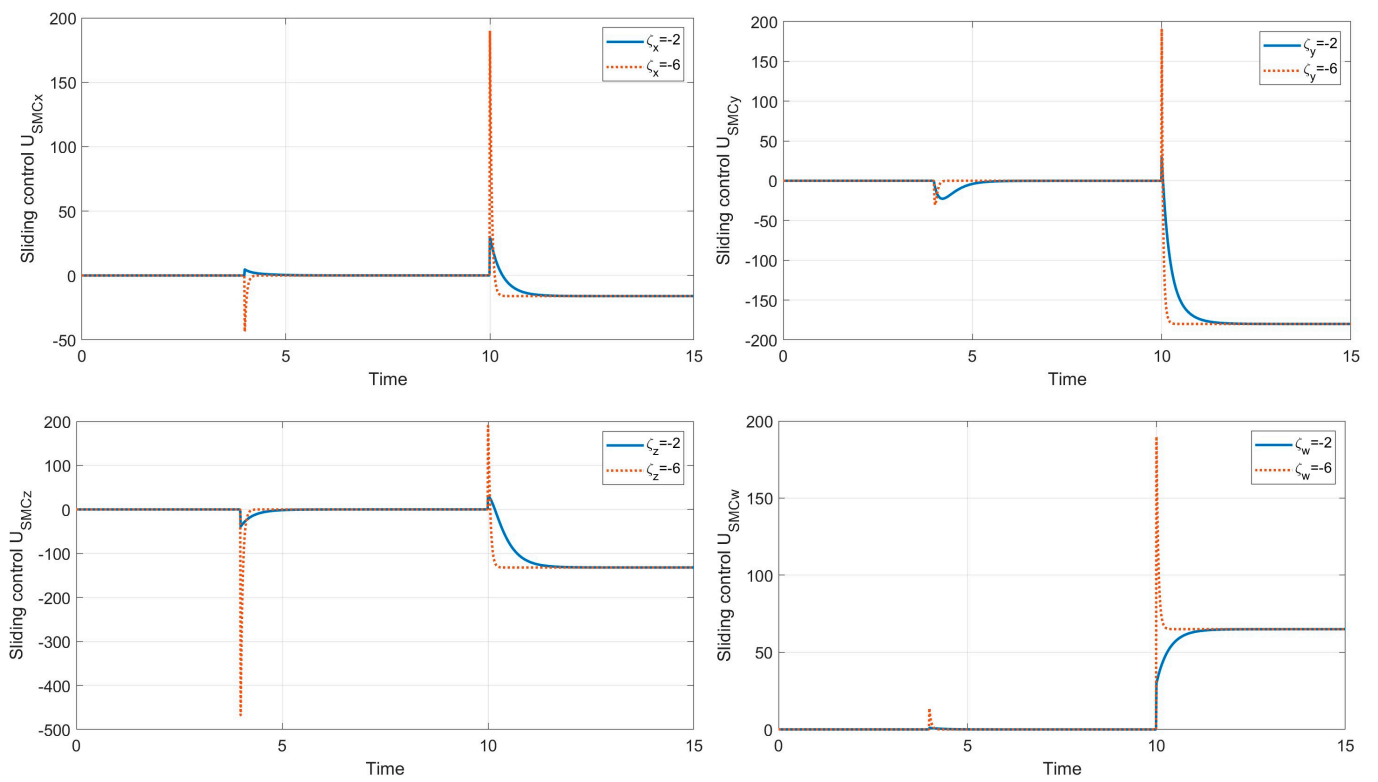


Figure 15. The behavior of the sliding model controller for removing chaotic supply chain behavior with changing values $\zeta_x, \zeta_y, \zeta_z, \zeta_w$.

5. Conclusions

This paper delves into the intricate dynamics of supply chains, highlighting the challenges posed by their interconnected components and susceptibility to disruptions. Our research utilized dynamical and multistability analyses to explore nonlinear behaviors and identify potential risks within these systems. Key findings from our dynamical analysis demonstrated how transport risk, quality risk, distortion, contingency reserves, and safety stock impact supply chain management. Each of these factors was shown to influence the stability and efficiency of supply chain operations significantly. Moreover, we introduced a sliding method for computing the sliding surface and its derivative, along with the derivation of an equivalent control law. This method presents promising avenues for controlling supply chain dynamics by providing a robust mechanism to manage the complexities and nonlinearities inherent in supply chains. Our sliding mode controller was validated through simulations, which underscored its effectiveness in stabilizing supply chain operations and enhancing performance. In practical terms, this controller can be implemented in supply chain management software and systems to automatically adjust key parameters such as order quantities, inventory levels, and safety stock in response to real-time data. Due to computational limitations, real applications will be implemented in future research.

Author Contributions: Conceptualization, M.D.J. and A.S.; Formal analysis, S.V. and K.B.; Funding acquisition, M.D.J.; Investigation, S.M.H., K.B. and S.V.; Methodology, S.M.H., M.H. and M.D.J.; Writing—original draft, M.D.J., A.S. and S.M.H.; writing—review and editing and supervision, K.B., M.H., S.V. and A.S. All authors have read and agreed to the published version of the manuscript.

Funding: This research was funded by Universitas Padjadjaran.

Data Availability Statement: Our manuscript has no associated data.

Conflicts of Interest: The authors declare that they have no conflicts of interest.

References

1. Bidhandi, H.M.; Yusuff, R.M.; Ahmad, M.M.H.M.; Bakar, M.R.A. Development of a new approach for deterministic supply chain network design. *Eur. J. Oper. Res.* **2009**, *198*, 121–128. [\[CrossRef\]](#)
2. Biswas, P.; Kumar, S.; Jain, V.; Chandra, C. Measuring supply chain reconfigurability using integrated and deterministic assessment models. *J. Manuf. Syst.* **2019**, *52*, 172–183. [\[CrossRef\]](#)
3. Göksu, A.; Kocamaz, U.E.; Uyaroglu, Y. Synchronization and control of chaos in supply chain management. *Comput. Ind. Eng.* **2015**, *86*, 107–115. [\[CrossRef\]](#)
4. Stapleton, D.; Hanna, J.B.; Ross, J.R. Enhancing supply chain solutions with the application of chaos theory. *Supply Chain Manag. Int. J.* **2006**, *11*, 108–114. [\[CrossRef\]](#)
5. Wang, J.; Chi, D.; Wu, J.; Lu, H.Y. Chaotic time series method combined with particle swarm optimization and trend adjustment for electricity demand forecasting. *Expert Syst. Appl.* **2011**, *38*, 8419–8429. [\[CrossRef\]](#)
6. Yuan, X. Understanding complex dynamics in inventory management with endogenous demand under social interactions: A chaos perspective. *Int. J. Syst. Sci. Oper. Logist.* **2023**, *10*, 2225715.
7. Chryssolouris, G.; Giannelos, N.; Papakostas, N.; Mourtzis, D. Chaos theory in production scheduling. *CIRP Ann.* **2004**, *53*, 381–383. [\[CrossRef\]](#)
8. Lu, J.C.; Nie, X.Y. Logistics distribution path optimization research based on adaptive chaotic disturbance flies optimization algorithm. In *IOP Conference Series: Earth and Environmental Science*; IOP Publishing: Bristol, UK, 2019; Volume 237, p. 052068.
9. Norouzi Nav, H.; Jahed Motlagh, M.R.; Makui, A. Robust controlling of chaotic behavior in supply chain networks. *J. Oper. Res. Soc.* **2017**, *68*, 711–724. [\[CrossRef\]](#)
10. Ma, J.; Ren, H.; Yu, M.; Zhu, M. Research on the complexity and chaos control about a closed-loop supply chain with dual-channel recycling and uncertain consumer perception. *Complexity* **2018**, *2018*, 1–13. [\[CrossRef\]](#)
11. Guo, Y.; Ma, J. Research on game model and complexity of retailer collecting and selling in closed-loop supply chain. *Appl. Math. Model.* **2013**, *37*, 5047–5058. [\[CrossRef\]](#)
12. Açıkgöz, N.; Çağıl, G.; Uyaroglu, Y. The experimental analysis on safety stock effect of chaotic supply chain attractor. *Comput. Ind. Eng.* **2020**, *150*, 106881. [\[CrossRef\]](#)
13. Hwang, H.B.; Xie, N. Understanding supply chain dynamics: A chaos perspective. *Eur. J. Oper. Res.* **2008**, *184*, 1163–1178. [\[CrossRef\]](#)

14. Anne, K.R.; Chedjou, J.C.; Kyamakya, K. Bifurcation analysis and synchronisation issues in a three-echelon supply chain. *Int. J. Logist. Res. Appl.* **2009**, *12*, 347–362. [[CrossRef](#)]
15. Mondal, S. A new supply chain model and its synchronization behaviour. *Chaos Solitons Fractals* **2019**, *123*, 140–148. [[CrossRef](#)]
16. Tirandaz, H. Complete synchronisation of supply chain system using adaptive integral sliding mode control method. *Int. J. Model. Identif. Control* **2019**, *31*, 314–322. [[CrossRef](#)]
17. Luo, Y.; Deng, F.; Ling, Z.; Cheng, Z. Local H_∞ synchronization of uncertain complex networks via non-fragile state feedback control. *Math. Comput. Simul.* **2019**, *155*, 335–346. [[CrossRef](#)]
18. Xu, X.; Lee, S.D.; Kim, H.S.; You, S.S. Management and optimisation of chaotic supply chain system using adaptive sliding mode control algorithm. *Int. J. Prod. Res.* **2021**, *59*, 2571–2587. [[CrossRef](#)]
19. Kocamaz, U.E.; Taşkın, H.; Uyaroglu, Y.; Göksu, A. Control and synchronization of chaotic supply chains using intelligent approaches. *Comput. Ind. Eng.* **2016**, *102*, 476–487. [[CrossRef](#)]
20. Hamidzadeh, S.M.; Rezaei, M.; Ranjbar-Bourani, M. Chaos synchronization for a class of uncertain chaotic supply chain and its control by ANFIS. *Int. J. Prod. Manag. Eng.* **2023**, *11*, 113–126. [[CrossRef](#)]
21. Nav, H.N.; Jahedmotlagh, M.R.; Makui, A. Robust H_∞ control for chaotic supply chain networks. *Turk. J. Electr. Eng. Comput. Sci.* **2017**, *25*, 3623–3636.
22. Liu, Z.; Jahanshahi, H.; Volos, C.; Bekiros, S.; He, S.; Alassafi, M.O.; Ahmad, A.M. Distributed consensus tracking control of chaotic multi-agent supply chain network: A new fault-tolerant, finite-time, and chatter-free approach. *Entropy* **2021**, *24*, 33. [[CrossRef](#)] [[PubMed](#)]
23. Shi, L.; Guo, W.; Wang, L.; Bekiros, S.; Alsubaie, H.; Alotaibi, A.; Jahanshahi, H. Stochastic Fixed-Time Tracking Control for the Chaotic Multi-Agent-Based Supply Chain Networks with Nonlinear Communication. *Electronics* **2022**, *12*, 83. [[CrossRef](#)]
24. Yan-Chen, W.; De-Gang, Z.; Xu, W. Prediction model of supply chain demand based on fuzzy neural network with chaotic time series. In Proceedings of the 2013 IEEE International Conference on Service Operations and Logistics, and Informatics, Dongguan, China, 28–30 July 2013; IEEE: New York, NY, USA, 2013; pp. 450–455.
25. Ngoc Cuong, T.; Xu, X.; Lee, S.D.; You, S.S. Dynamic analysis and management optimization for maritime supply chains using nonlinear control theory. *J. Int. Marit. Saf. Environ. Aff. Shipp.* **2020**, *4*, 48–55. [[CrossRef](#)]
26. Sepestanaki, M.A.; Rezaee, H.; Soofi, M.; Fayazi, H.; Rouhani, S.H.; Mobayen, S. Adaptive continuous barrier function-based super-twisting global sliding mode stabilizer for chaotic supply chain systems. *Chaos Solitons Fractals* **2024**, *182*, 114828. [[CrossRef](#)]
27. Hamidzadeh, S.M.; Rezaei, M.; Ranjbar-Buorani, M. Control and Synchronization of The Hyperchaotic Closedloop Supply Chain Network by PI Sliding Mode Control. *Int. J. Ind. Eng. Prod. Res.* **2022**, *33*, 1–13.
28. Johansyah, M.D.; Sambas, A.; Mobayen, S.; Vaseghi, B.; Al-Azzawi, S.F.; Sukono; Sulaiman, I.M. Dynamical analysis and adaptive finite-time sliding mode control approach of the financial fractional-order chaotic system. *Mathematics* **2022**, *11*, 100. [[CrossRef](#)]
29. Ramírez, S.A.; Peña, G. Analysis of chaotic behaviour in supply chain variables. *J. Econ. Financ. Adm. Sci.* **2011**, *16*, 85.
30. Ma, J.; Xie, L. The impact of loss sensitivity on a mobile phone supply chain system stability based on the chaos theory. *Commun. Nonlinear Sci. Numer. Simul.* **2018**, *55*, 194–205. [[CrossRef](#)]
31. Cuong, T.N.; Kim, H.S.; You, S.S. Decision support system for managing multi-echelon supply chain networks against disruptions using adaptive fractional order control algorithm. *RAIRO-Oper. Res.* **2023**, *57*, 787–815. [[CrossRef](#)]
32. Pellegrino, R.; Costantino, N.; Tauro, D. The value of flexibility in mitigating supply chain transportation risks. *Int. J. Prod. Res.* **2021**, *59*, 6252–6269. [[CrossRef](#)]
33. Liu, C.H.; Xiong, W. Modelling and simulation of quality risk forecasting in a supply chain. *Int. J. Simul. Model.* **2015**, *2*, 359–370. [[CrossRef](#)]
34. Ma, J.; Lou, W.; Tian, Y. Bullwhip effect and complexity analysis in a multi-channel supply chain considering price game with discount sensitivity. *Int. J. Prod. Res.* **2019**, *57*, 5432–5452. [[CrossRef](#)]
35. Dominguez, R.; Cannella, S.; Framinan, J.M. The impact of the supply chain structure on bullwhip effect. *Appl. Math. Model.* **2015**, *39*, 7309–7325. [[CrossRef](#)]
36. Lücker, F.; Seifert, R.W.; Biçer, I. Roles of inventory and reserve capacity in mitigating supply chain disruption risk. *Int. J. Prod. Res.* **2019**, *57*, 1238–1249. [[CrossRef](#)]
37. Wei, Y.; Wang, H.; Qi, C. The impact of stock-dependent demand on supply chain dynamics. *Appl. Math. Model.* **2013**, *37*, 8348–8362. [[CrossRef](#)]
38. Al-Azzawi, S.F.; Al-Hayali, M.A. Multistability and hidden attractors in a novel simple 5D chaotic Sprott E system without equilibrium points. *J. Interdiscip. Math.* **2022**, *25*, 1279–1294. [[CrossRef](#)]
39. Al-hayali, M.A.; Al-Azzawi, F.S. A 4D hyperchaotic Sprott S system with multistability and hidden attractors. *J. Phys. Conf. Ser.* **2021**, *1879*, 032031. [[CrossRef](#)]
40. Benkouider, K.; Vaidyanathan, S.; Sambas, A.; Tlelo-Cuautle, E.; Abd El-Latif, A.A.; Abd-El-Atty, B.; Kumam, P. A new 5-D multistable hyperchaotic system with three positive Lyapunov exponents: Bifurcation analysis, circuit design, FPGA realization and image encryption. *IEEE Access* **2022**, *10*, 90111–90132. [[CrossRef](#)]
41. Sambas, A.; Miroslav, M.; Vaidyanathan, S.; Ovilla-Martínez, B.; Tlelo-Cuautle, E.; Abd El-Latif, A.A.; Bonny, T. A New Hyperjerk System with a Half Line Equilibrium: Multistability, Period Doubling Reversals, Antimonotonicity, Electronic Circuit, FPGA Design and an Application to Image Encryption. *IEEE Access* **2024**, *12*, 9177–9194. [[CrossRef](#)]

42. Sambas, A.; Vaidyanathan, S.; Zhang, X.; Koyuncu, I.; Bonny, T.; Tuna, M.; Kumam, P. A novel 3D chaotic system with line equilibrium: Multistability, integral sliding mode control, electronic circuit, FPGA implementation and its image encryption. *IEEE Access* **2022**, *10*, 68057–68074. [[CrossRef](#)]
43. Cuong, T.N.; Kim, H.S.; Nguyen, D.A.; You, S.S. Nonlinear analysis and active management of production-distribution in nonlinear supply chain model using sliding mode control theory. *Appl. Math. Model.* **2021**, *97*, 418–437. [[CrossRef](#)]

Disclaimer/Publisher’s Note: The statements, opinions and data contained in all publications are solely those of the individual author(s) and contributor(s) and not of MDPI and/or the editor(s). MDPI and/or the editor(s) disclaim responsibility for any injury to people or property resulting from any ideas, methods, instructions or products referred to in the content.